Large-Scale Fabrication of Protein Nanoarrays Based on Nanosphere Lithography

Yuguang Cai* and Benjamin M. Ocko*

Physics Department, Brookhaven National Laboratory, Upton, New York 11973

Received June 20, 2005

Hexagonally patterned lysozyme nanoarrays have been assembled on silicon wafers by combining nanosphere lithography and surface silane chemistry using vapor and solution deposition processes. The patterned protein regions extend over cm sized regions, and the size of each island is ∼120 nm for the solution-prepared template and ∼60 nm for the vapor-prepared template. Antibody test indicates that the patterned lysozyme maintains its bioactivity on the surface. This new approach offers a fast and reliable method to fabricate protein arrays over large areas with feature sizes comparable to scanning-probe based techniques.

Introduction

Developing nanoscale protein arrays is an important step toward many emerging biological and medical applications.[1] Miniaturization of protein arrays provides high array densities, which reduce the amount of analytes required and minimizes the fabrication and analysis cost. Also, miniaturization has the potential to improve the performance of biosensors by providing better sensitivity and signal quality. Further, reducing the size of protein islands into the nanometer regime offers a new approach toward investigating specific biological reactions through novel detecting methods such as surface enhanced raman spectroscopy (SERS).[2,3] Additionally, nanoscale protein patterning is an important prerequisite for fabricating novel protein devices such as nanopropellers and protein diode.[4,5]

Dip-pen lithography,[6] nanografting,[7−10] and conducting tip AFM writing[11,12] are emerging scanning probe-based lithographies that are capable of creating nanopatterns with sub-100 nm resolution over small surface regions. All of these methods have been used to create protein patterns. Patterning techniques, such as photolithography[13,14] and laser lithography[15] are used to pattern proteins over large area, but they lack the nanoscale resolution. Microcontact printing (μCP) and nanoimprinting have the potential for creating complicated large-scale protein patterns with sub-100 nm resolution but both methods require specialized stamps.[1,16,17] Here we demonstrate a simple nanosphere based lithography method to direct the assembly of proteins into arrays of ∼100 nm islands over macroscopic surface areas. In nanosphere lithography, also known as natural lithography[18] or colloidal lithography,[19] the self-assembly of a nanosphere monolayer on a solid surface provides a simple and effective means of creating a hexagonally patterned lithographic mask for further surface processing. The geometry of the spheres restricts deposition processes and prevents chemical modification directly beneath the nanospheres. As such, nanosphere lithographic patterns have been employed to create metal clusters arrays,[20] to form negative-toned protein patterns[21] and nano-rings on the surface.[22] In the present study, we utilize both nanosphere lithography and silane chemistry[23] to chemically pattern surfaces with a regular array of sub-100 nm islands over cm sample regions. These chemically patterned regions are used as a template to selectively adsorb lysozyme on carboxylic acid terminated islands and not on the interstitial regions between the islands. In this manner, positive-toned protein nanoarrays are fabricated. The lysozyme nanoarrays maintain their bioactivity on the surface as evidenced by their high sensitivity toward the antibody.

Experimental Section

In this study, we have used the protein lysozyme since it is readily available and its structure and properties are well-known. Lysozyme is positively charged in a pH 7 solution since it has an isoelectric point of 11 and it will selectively adsorb on the

* To whom correspondence should be addressed. E-mail: ycai@bnl.gov (Y.C.); ocko@bnl.gov (B.M.O.).

(1) Kane, R. S.; Takayama, S.; Ostuni, E.; Ingber, D. E.; Whitesides, G. M. *Biometerials* **1999**, *20*, 2363.
(2) Xu, H. X.; Bjerneld, E. J.; Kall, M.; Borjesson, L. *Phys. Rev. Lett.* **1999**, *83*, 4357.
(3) Haes, A. J.; Chang, L.; Klein, W. L.; Van Duyne, R. P. *J. Am. Chem. Soc.* **2005**, *127*, 2264.
(4) Soong, R. K.; Bachand, G. D.; Neves, H. P.; Olkhovets, A. G.; Craighead, H. G.; Montemagno, C. D. *Science* **2000**, *290*, 1555.
(5) Rinaldi, R.; Biasco, A.; Maruccio, G.; Arima, V.; Visconti, P.; Cingolani, R.; Facci, P.; De Rienzo, F.; Di Felice, R.; Molinari, E.; Verbeet, M. P.; Canters, G. W. *Appl. Phys. Lett.* **2003**, *82*, 472.
(6) Lee, K. B.; Park, S. J.; Mirkin, C. A.; Smith, J. C.; Mrksich, M. *Science* **2002**, *295*, 1702.
(7) Cheung, C. L.; Camarero, J. A.; Woods, B. W.; Lin, T. W.; Johnson, J. E.; De Yoreo, J. J. *J. Am. Chem. Soc.* **2003**, *125*, 6848.
(8) Liu, G. Y.; Amro, N. A. *P. Natl. Acad. Sci. U.S.A.* **2002**, *99*, 5165.
(9) Case, M. A.; McLendon, G. L.; Hu, Y.; Vanderlick, T. K.; Scoles, G. *Nano Lett.* **2003**, *3*, 425.
(10) Kenseth, J. R.; Harnisch, J. A.; Jones, V. W.; Porter, M. D. *Langmuir* **2001**, *17*, 4105.
(11) Pavlovic, E.; Oscarsson, S.; Quist, A. P. *Nano Lett.* **2003**, *3*, 779.
(12) Gu, J. H.; Yam, C. M.; Li, S.; Cai, C. Z. *J. Am. Chem. Soc.* **2004**, *126*, 8098.
(13) Mooney, J. F.; Hunt, A. J.; McIntosh, J. R.; Liberko, C. A.; Walba, D. M.; Rogers, C. T. *P. Natl. Acad. Sci. U.S.A.* **1996**, *93*, 12287.
(14) Yap, F. L.; Zhang, Y. *Langmuir* **2005**, *21*, 5233.
(15) Shivashankar, G. V.; Libchaber, A. *Appl. Phys. Lett.* **1998**, *73*, 417.
(16) Chou, S. Y.; Krauss, P. R.; Renstrom, P. J. *J. Vac. Sci., Technol. B* **1996**, *14*, 4129.
(17) Hoff, D. J.; Cheng, L. J.; Meyhõfer, E.; Guo, L. J. Hunt, A. J. *Nano Lett.* **2004**, *4*, 853.
(18) Deckman, H. W.; Dunsmuir, J. H. *Appl. Phys. Lett.* **1982**, *41*, 377.
(19) Denis, F. A.; Hanarp, P.; Sutherland, D. S.; Gold, J.; Mustin, C.; Rouxhet, P. G.; Dufrene, Y. F. *Langmuir* **2002**, *18*, 819.
(20) Haynes, C. L.; Van Duyne, R. P. *J. Phys. Chem. B* **2001**, *105*, 5599.
(21) Garno, J. C.; Amro, N. A.; Wadu-Mesthrige, K.; Liu, G. Y. *Langmuir* **2002**, *18*, 8186.
(22) Wang, Y.; Han, S. B.; Briseno, A. L.; Sanedrin, R. J. G.; Zhou, F. M. *J. Mater. Chem.* **2004**, *14*, 3488.
(23) Buriak, J. M. *Chem. Rev.* **2002**, *102*, 1271.

10.1021/la051656e CCC: $30.25 © 2005 American Chemical Society
Published on Web 08/27/2005

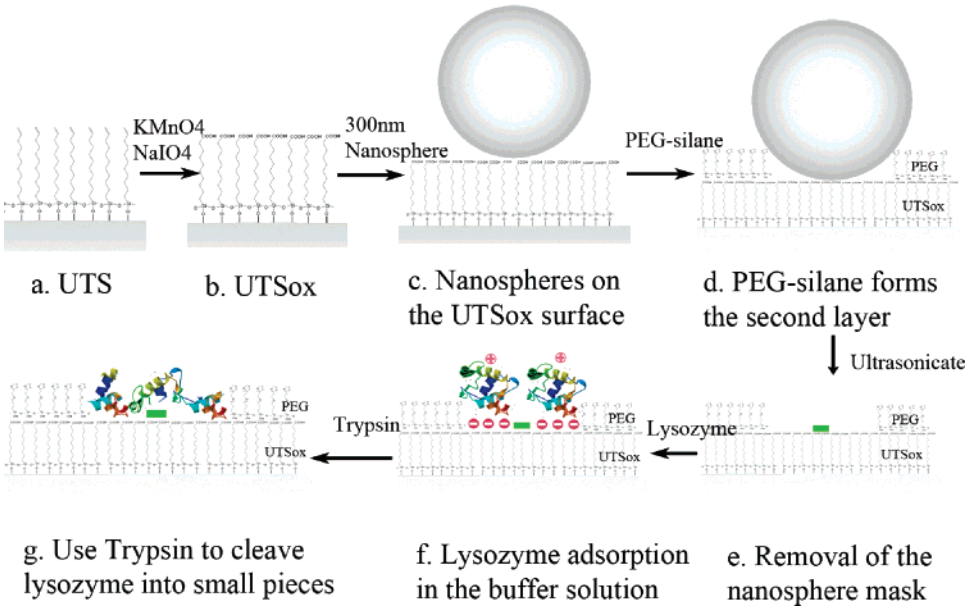

Figure 1. Nanopatterned protein deposition scheme using liquid phase PEG-silane deposition. (a) Deposit a UTS monolayer from in BCH solution. (b) Oxidize the terminal double bond to carboxylic group in $KMnO_4/NaIO_4$ solution, forming a hydrophilic UTS_{ox} surface. (c) Deposit a 300 nm nanosphere on the UTS_{ox} surface, thus forming a polycrystalline monolayer mask over the whole sample (1×1 cm^2). (d) Deposit a PEG-silane, second layer. (e) Ultrasonic removal of nanospheres. The green bar left at the sphere−UTS_{ox} surface contact point is a residue of the polystyrene nanosphere. (f) Deposit lysozyme onto the surface in a pH 7 HEPES buffer. The protein selectively adsorbs on the patterned UTS_{ox} holes. (g) Treat the protein pattern with trypsin, which specifically cuts the peptide bond after arginine and lysine. The lysozyme is cleaved into several small pieces. The protein islands disappear.

negatively charged carboxylic acid terminated regions. Nanosphere monolayer masks along with silane chemistry have been utilized to fabricate a carboxylic terminated, hexagonal packed chemical pattern. The hexagonally packed nanosphere mask is assembled on a carboxylic terminated silane monolayer. Then octadecyltrichlorosilane (OTS) or poly(ethylene glycol) silane (PEG-silane) is deposited, and these silane molecules only attach to the hydrophilic carboxylic terminated regions between the spheres and not directly under the spheres. After removing the mask, a hexagonal array of COOH terminated holes is formed.

Materials and Instruments. 2-[Methoxy(polyethylenoxy)-propyl] tricholorosilane (PEG-silane) and 10-undecenyltricholorosilane (UTS) are from Gelest. Bicyclohexyl (BCH), octadecyltrichlorosilane (OTS), and sodium periodate were obtained from Sigma-Aldrich. The 300 nm polystyrene nanosphere, 1 wt % solution (Duke Scientific, Inc.) was centrifuged three times at 10 000 *g* to remove the surfactant. The lysozyme antibody (Hen egg white, rabbit) is from the Rockland Immunochemicals, Inc**.** The silane surface contact angle was measured using a Data-Physics OCA contact angle instrument. AFM images were acquired using a Molecular Imaging PicoPlus AFM in both contact and tapping mode.

Pattern Fabrication. We used two slightly different routes to fabricate chemical patterns after assembling the nanosphere mask. In the first route, the nanopatterned silane layer is formed via solution phase deposition, whereas in the second route, the nanopatterned silane layer is formed via vapor phase deposition. The step-by-step solution-based nanopatterning scheme is illustrated in Figure 1.

A monolayer of UTS was deposited on pirahna-cleaned silicon wafers (1×1 cm^2) using a 5 mM UTS BCH solution. The UTS coated surface appeared hydrophobic with a water contact angle of $99 \pm 2°$. To convert the terminal double bond to COOH, the sample was dipped into a solution containing 5×10^{-4} M $KMnO_4$ and 0.02 M $NaIO_4$ and incubated at 40 °C for 10 h.[24] To remove remnant permanganate or MnO_2, the wafer was rinsed in a 1 mM hydrazine solution for 1 min. As prepared, the surface is hydrophilic, suggesting that the existence of the COOH terminated C10 silane (referred to in the following as UTS_{ox}) film on the surface. To test this hypothesis, the hydrophilic substrate was placed in a 5mM OTS BCH solution overnight to see if a second layer forms above the UTS_{ox} surface. After rinsing with toluene, the organic layer thickness was measured with X-ray reflectivity. The X-ray spectrum shows the existence of a 4.0 nm thick film, corresponding to the sum of the heights of OTS film (2.5 nm)[25] and UTS_{ox} film (1.4 nm).[26] The hydrophilic nature of the surface after the surface oxidation and the thickness of the bilayer film indicate the existence of a UTS_{ox} surface after the oxidative reaction. To deposit a monolayer of nanospheres, a thin layer of 1.5 μL 1% nanosphere aqueous solution was applied to the dried UTS_{ox} surface and allowed to slowly evaporate. At this stage, the AFM images showed that the nanospheres form an ordered, hexagonally closed-packed monolayer over the entire surface region.

Previous studies have shown that an organic bilayer film can be formed starting with a monolayer prepared with a molecule similar to UTS but with eight additional CH_2 units, referred to as NTS by Sagiv and Maoz. This has been accomplished for the monolayer prepared with NTS by first oxidizing the terminal double bond and then dipping the surface into a solution containing OTS.[27] We have used a similar procedure to fabricate double layers using UTS_{ox} (10 carbon atoms) rather than NTS_{ox} (18 carbon atoms) where the silanes were either solution or vapor deposited. In the solution deposition case, the second layer is formed through dipping the nanosphere masked UTS_{ox} surface into a PEG-silane BCH solution. Since the surface is coated by a monolayer of nanospheres, the PEG-silane does not attach to the parts of surface that are directly underneath the nanospheres. The alternative patterning fabrication procedure is to use vapor deposition to form the second layer silane above the UTS_{ox}. In this case, the patterning fabrication scheme is similar to the scheme of the solution-based route (Figure 1) except that the PEG-silane BCH solution is replaced by the OTS silane vapor which then reacts with the UTS_{ox} substrate. The wafer with the nanosphere mask is placed in a sealed container with a beaker of 2 mL of OTS. The sample is incubated for 12 h at 60 °C in order to sufficiently increase the vapor pressure of the OTS. Under these conditions, the OTS molecules grow between the nanospheres and form a second layer above the UTS_{ox} monolayer. For

(24) Wasserman, S. R.; Tao, Y. T.; Whitesides, G. M. *Langmuir* **1989**, *5*, 1074.
(25) Tillman, N.; Ulman, A.; Schildkraut, J. S.; Penner, T. L. *J. Am. Chem. Soc.* **1988**, *110*, 6136.
(26) Calculated value based on the UTS film thickness (1.5 nm) in ref 25.
(27) Maoz, R.; Sagiv, J. *Adv. Mater.* **1998**, *10*, 580.

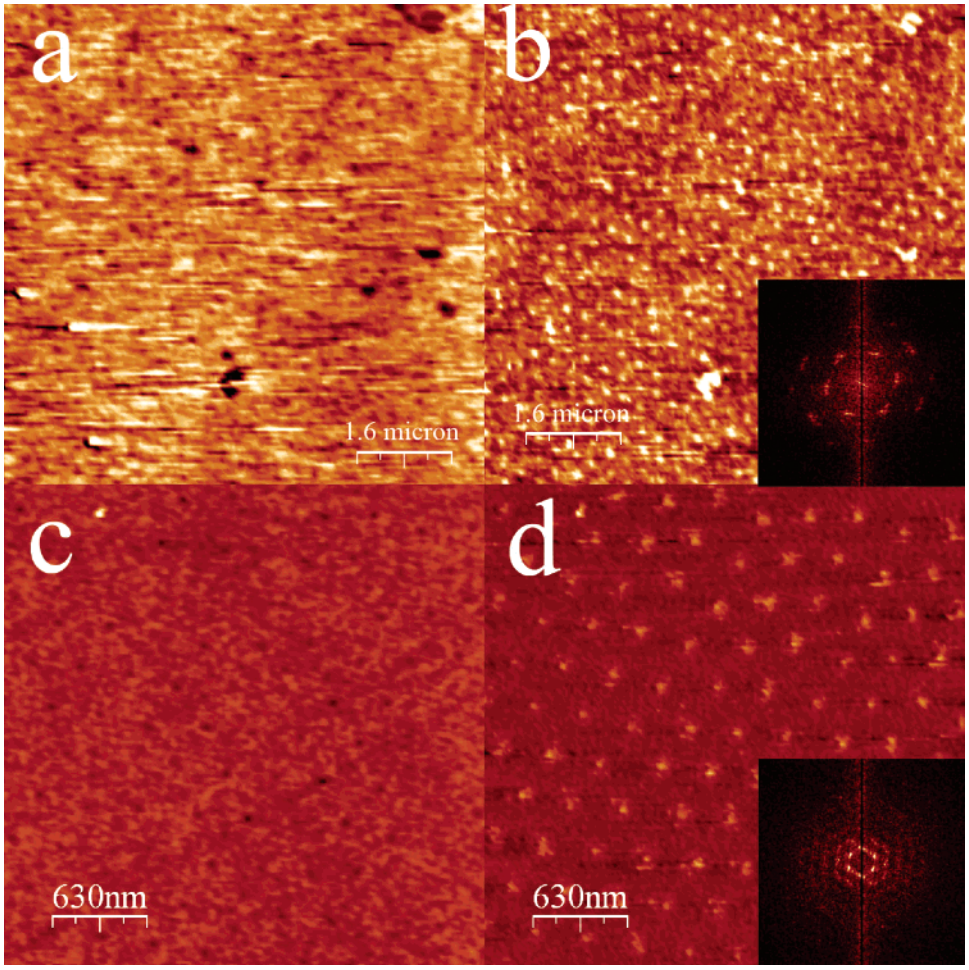

Figure 2. AFM Images of the fabricated templates of hexagonally packed UTS_{ox} Holes. (a) Topography and (b) friction images of the solution-prepared UTS_{ox}−PEG silane surface. ($8 \times 8\ \mu m^2$). (c) Topography and (d) friction images of the vapor-phase-prepared UTS_{ox}−OTS surface silane surface ($4.38 \times 4.38\ \mu m^2$). Brighter contrast in topography images corresponds to higher surface height; and higher friction force in friction images. In panel b and d, the hydrophilic UTS_{ox} terminus appears as bright spots, indicating a higher friction when imaged by a hydrophilic tip. The insets in (b) and (d) are the Fourier transformed images of (b) and (d). The hexagonal order is clearly observed in both templates.

both vapor and solution deposition methods, after removing the nanospheres by ultrasonication in water, the surfaces appear to be patterned with carboxylic terminated hexagonally packed UTS_{ox} holes that are surrounded by a second layer composed of either the PEG-silane or OTS.

Protein Adsorption. To deposit the protein on the UTS_{ox}-PEG silane surface, one drop of a 4μg/mL lysozyme solution in a 25 mM pH = 7, HEPES buffer is applied. The protein solution is then removed after 5 min with a burst of compressed nitrogen, and the surface is subsequently rinsed with a 25 mM pH7 HEPES buffer solution. The excessive solution was removed by touching a paper towel to the edge of the substrate. To deposit the protein on the vapor-prepared OTS−UTS_{ox} surface, a slightly different deposition scheme is used, which appears to yield more reproducible results on this surface. One drop of a 25 ng/mL lysozyme solution is applied on the surface for 5 min. The excessive solution was also removed using a paper towel and soaked in 1:400 Tween surfactant solution for 25 min. The removal of excessive solution and the soaking cycle was repeated three times to remove excessive protein.

Compared with the carboxylic terminated surface, the lower surface energy PEG- and methyl-terminated surfaces have lower affinities toward protein adsorption.[28] Based on the electrostatic interactions of a pH = 7 buffer solution, the positively charge lysozyme (isoelectric point of 11) should adsorb in the negatively charged, carboxylic terminated UTS_{ox} holes (Figure 1f). The AFM imaging is carried out under 100% relative humidity to avoid protein denaturing. Both surfaces are imaged by AFM immediately after the protein depositions are complete.

Results and Discussion

The lysozyme nanoarray fabrication process is composed of several steps including mask preparation, surface reactions and protein deposition. The quality of each stage of the processing clearly affects the outcome of the subsequent stages. Thus, we have monitored the structure of the templates at each step, and we have optimized the preparation conditions to obtain the best quality patterned surfaces.

The first step in the protein nanoarray fabrication process is the preparation of the nanosphere mask. The close packing of the colloidal 300 nm nanospheres produces a hexagonally ordered mask which is used for further silane chemistry and protein adsorption. The order, coverage, stability, and defect density of the mask determine the quality of the protein pattern. By using a relatively slow solution evaporation rate, we obtained reasonably uniform monolayers of the polystyrene nanosphere covering the entire wafer ($1 \times 1\ cm^2$). The typical crystalline domain size of the sphere is approximately $30 \times 30\ \mu m^2$, which contains ~10 000 individual polystyrene spheres. In the Supporting Information, Figure S1a, we show an AFM image of a typical nanosphere single crystal domain. The FFT image in Figure S1b indicates that it is well ordered.

(28) Sharma, S.; Popat, K. C.; Desai, T. A. *Langmuir* **2002**, *18*, 8728.

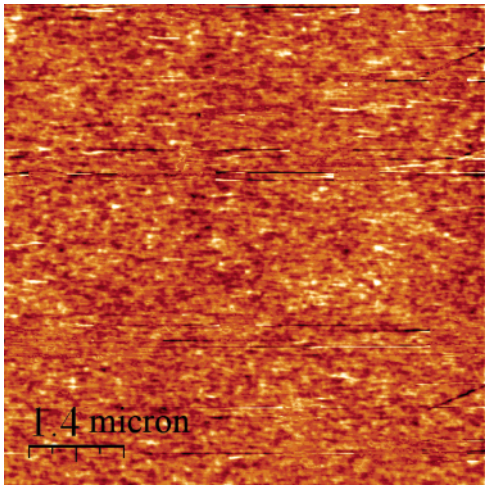

Figure 3. UTS_{ox}−PEG-silane surface after treated with trypsin. The hexagonal packed islands disappear, leaving a featureless surface. Lateral scale is $7 \times 7\ \mu m^2$, and the z scale is 1.4 nm.

Figure 2 shows the AFM contact mode images of the fabricated patterned surfaces of the solution-prepared UTS_{ox}−PEG silane (Figure 2, panels a and b) and the vapor-phase-prepared UTS_{ox}−OTS(Figure 2, panels c and d). These images were obtained after forming the second silane layer and removing the polystyrene sphere mask. Whereas the topographic images (Figure 2, panels a and c) are not clearly observable, friction images (Figure 2, panels b and d) clearly exhibit hexagonally arranged, carboxylic UTS_{ox} holes. These images also demonstrate the crystalline-like order of the nanosphere patterns. In these friction images, the UTS_{ox} holes appear as white spots (higher friction). The higher friction of the UTS_{ox} regions, compared to the surrounding OTS or PEG-silane regions, is due to the higher attractive interaction between the hydrophilic tip scanning over the hydrophilic carboxyl terminated UTS_{ox} holes compared to the non-hydrophillic regions. The AFM images in Figure 2 illustrate the hexagonal chemical patterns on both templates. These patterns are the precursors of the protein patterns described below.

The AFM images shown in Figure 4 in topography (a) and friction (b) modes show the existence of hexagonally packed lysozyme islands with a 300 nm spacing. These templates were prepared from solution using UTS_{ox}−PEG, as described above. Similarly, panel c shows the vapor-

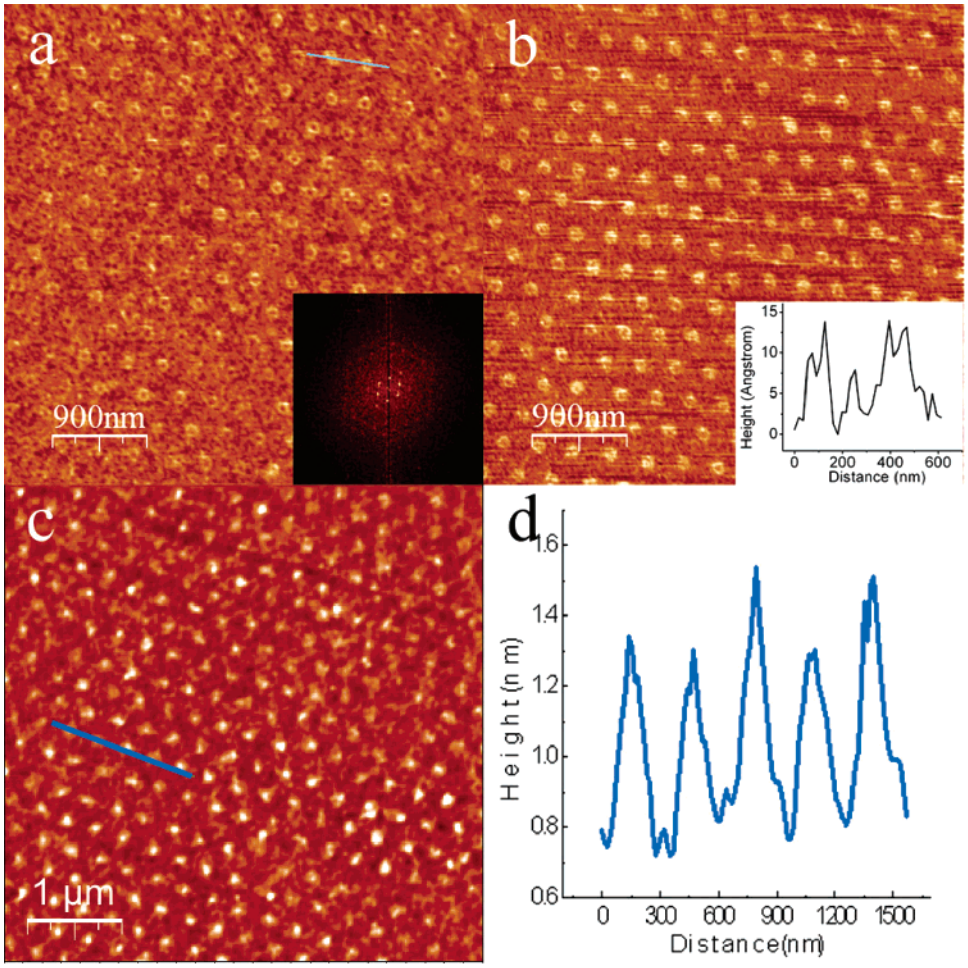

Figure 4. Lysozyme pattern on the solution-prepared UTS_{ox}−PEG silane surface (a and b) and the vapor-phase-prepared UTS_{ox}−OTS surface (c). (a) Topographical and (b) friction mode images the island−island distance is 300 nm. The island is ring shaped with an outer ring diameter of 118 ± 6 nm. The ring width is about 50 nm. The inset in (a) shows the Fourier transform of the image in (a). In the friction mode image (b), the brighter color corresponds to higher friction force. The higher friction of the protein islands shows the protein surface is hydrophilic. The inset shows the height profile corresponding to the blue line in (a), indicating the protein island is ~1.5 nm higher than the surrounding surface. The height measured from tapping mode image (not shown) shows similar value. (c) Tapping mode topographic image of lysozyme nanoarrays on the vapor-phase-prepared UTS_{ox}−OTS surface. The island size is measured to be 61 ± 4 nm. (d) Height profile of the blue line in (c) indicates the lysozyme island is ~0.4 nm higher than the surrounding OTS surface.

phase-prepared UTS_{ox}−OTS surface after lysozyme adsorption. In the topography images for both samples, the surface evolves from a surface with negative depressions prior to protein adsorption to a surface with positive protrusions after protein adsorption. These images clearly demonstrate that the lysozyme molecules indeed adsorb on the carboxylic terminated holes. Further details on the solution-prepared protein nanoarrays, including the presence of highly ordered hexagonal arrays, are shown in Figure S2 of the Supporting Information. To obtain accurate information about the surface properties including the height of the pattern features, both surfaces are imaged in contact mode and tapping mode AFM. In the friction images of Figure 4a, the protein islands also exhibit a relatively high friction force when imaged with a hydrophilic silicon nitride tip. This is not surprising since lysozyme is a water-soluble protein with a hydrophilic surface. Measured with AFM tapping mode, the protein islands on the vapor-phase-prepared UTS_{ox}−OTS template are ~0.4 nm higher than the OTS surface (see Figure 4d), whereas the protein islands on the solution-prepared UTS_{ox}−PEG silane surface appear to be 1−1.5 nm higher than the surrounding PEG-silane surface. Since the OTS and PEG-silane films respectively have heights of 2.5 and 1.5−1.7 nm,[29] we infer that the heights of the protein immobilized inside the UTS_{ox} hole on both templates are each about 3 nm high. Considering the dimension of lysozyme (5 × 3 × 3 nm), the height in the protein nanoarrays suggests that the lysozyme adsorbs on the surface with its long axis parallel to the surface.

Although the lysozyme heights are similar for both templates, there are important differences in the protein nanoarrays prepared from the solution and vapor phases. For the solution-prepared UTS_{ox}−PEG-silane surface, the protein islands adopts a ring-like shape, with a ring diameter of 118 ± 6 nm and a ring width of ~50 nm (see Figure 3). Apparently, no protein adsorbs in the central region of the protein island, where the polystyrene nanosphere had contacted the surface. Thus, it appears that the nanospheres leave a "footprint" on the surface that prohibits protein adsorption. The AFM friction image reveals that the "footprint" has a low friction when imaged with a hydrophilic tip, indicating it has a hydrophobic nature. In contrast, the protein island is disk shaped, with a diameter of 61 ± 4 nm, on the vapor-phase-prepared UTS_{ox}−OTS surface. Based on this important difference, we infer that the "footprint" observed in the center of the ring on the solution-prepared template is related to the organic solvent (BCH) used in the preparation procedure. One possibility is that the BCH might dissolve a trace amount of the polystyrene sphere and deposit this material on the surface, leaving behind a hydrophobic "footprint". Similar processes such as the partial melting of the polystyrene spheres at elevated temperature also lead to "footprints" of colloidal polystyrene spheres on the surface.[20]

The size of the protein island appears to be determined by the size of the UTS_{ox} holes on the templates. For the vapor-prepared UTS_{ox}−OTS template, the size of the hole can be explained by a simple geometric model as described in the illustration in Figure 5. Considering the height of the OTS molecule (2.5 nm) and the radius of the polystyrene sphere (150 nm), there should be a 55 nm diameter hole that the deposited OTS molecules are not able to coat. This model is supported by the measured UTS_{ox} hole diameter of 61 ± 4 nm. The small difference

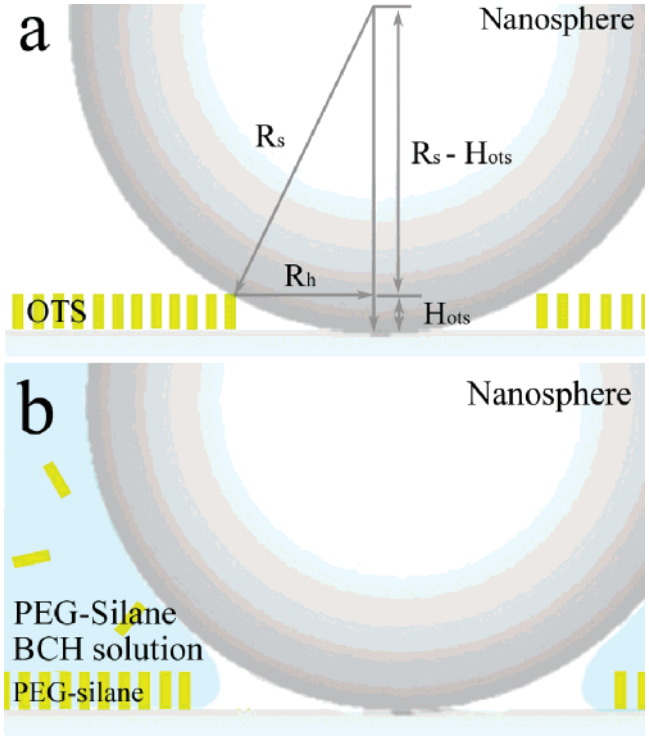

Figure 5. Origin of the UTS_{ox} hole. (a) In the vapor-phase-prepared UTS_{ox}−OTS template, the height of OTS molecules indicated that OTS molecules cannot grow directly under the nanosphere. The radius of this area (R_h) is calculated to be $R_h = R_s \sin(\arccos(R_s - H_{OTS}/R_s))$, where R_s is the radius of the nanosphere (150 nm) and H_{OTS} is the height of the OTS molecule (2.5 nm). (b) In the solution-prepared UTS_{ox}−PEG-silane template, there is a region with a ~120 nm diameter area that is not wet.

might be accounted for by the broadening affects of the ~20 nm sized AFM tip. On the other hand, this model cannot explain the measured 118 ± 6 nm protein island size of the solution-prepared surface. It is not obvious why the islands are larger on the liquid-phase-prepared template but a possible explanation might involve nanoscale effects of wetting.

To provide further proof that the hexagonal topographic protrusions on the template are from the lysozyme, additional control measurements were carried out. In the first experiment, a buffer solution without lysozyme was applied to the surface patterned with UTS_{ox} holes. AFM scans showed no topography change from the UTS_{ox}−PEG silane template. In the second experiment, the patterned surface was treated with 4μg/mL trypsin solution after lysozyme adsorption. Trypsin is well-known to specifically cut the peptide bond after arginine and lysine, both of which are abundant in lysozyme. Thus, the lysozyme should be cleaved into many small pieces as illustrated by the cartoon in Figure 1g. After this procedure, the AFM image shown in Figure 3 clearly indicates that the protrusion pattern exhibited prior to the typsin procedure (Figure 4a), has vanished. These controls provide further evidence that lysozyme was indeed deposited from the solution phase.

To probe the activity of the lysozyme nanoarrays, we carried out a lysozyme antibody test on the vapor-prepared UTS_{ox}−OTS template. This template has smaller lysozyme islands compared to the PEG-terminated surface and is lacking the ring "footprint" feature. These characteristics make the vapor-prepared UTS_{ox}−OTS template the preferred choice for the antibody test. As a control, a drop

(29) Papra, A.; Gadegaard, N.; Larsen, N. B. *Langmuir* **2001**, *17*, 1457.

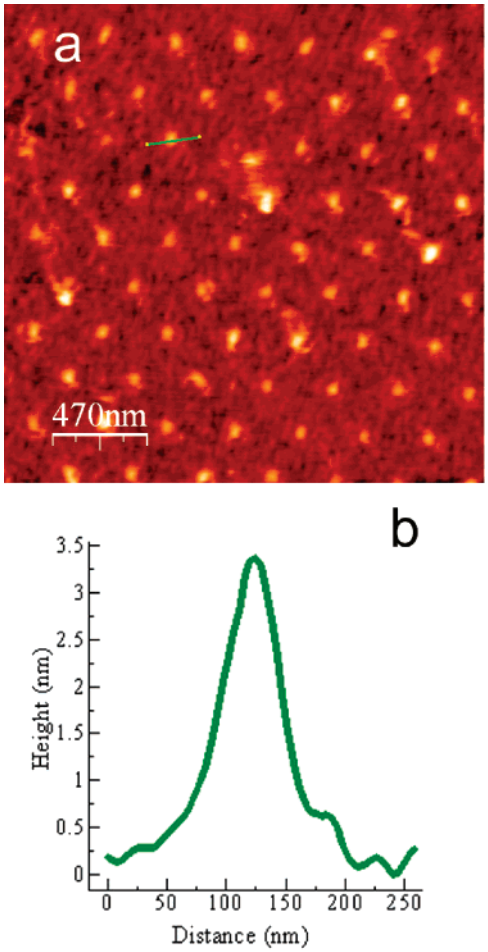

Figure 6. Lysozyme nanoarrays after the antibody adsorption. (a) Topographic image of the lysozyme nanoarrays after the antibody adsorption. The antibody only selectively adsorbs on the lysozyme islands and not on the surrounding OTS surface. (b) Height profile corresponds to the green line in (a). The height profile indicates that the height of the islands increase to 3.5 nm, which is 3 nm higher than the lysozyme island height before the antibody deposition.

of 700ng/mL rabbit anti-hen white lysozyme antibody in 3mM HEPES 7.4 buffer is applied for 30 min to a uniform OTS coated surface. AFM images (not shown) on this surface revealed that a small amount of the antibodies nonspecifically adsorbs on the OTS, and these antibodies appeared as isolated spots. The height of these antibody spots is measured to be ~3 nm. On the UTS_{ox}−OTS prepared protein array surface, a single drop (~30 μL) of a 100ng/mL rabbit anti-hen white lysozyme antibody in 3mM HEPES 7.4 buffer is applied. After 5 min, the surface is rinsed with 50 mM HEPES 7.4 solution twice and imaged by AFM in tapping mode. Figure 6 shows the height of the protein islands increased by an additional 3 nm. Indeed, this height is exactly the same as the antibody height measured in the control experiment. Since the antibody protein only adsorbed on the islands and since it was not adsorbed on the OTS background, we conclude that the adsorption of the antibody is through bio-recognition rather than nonspecific adsorption. Thus, we infer that the lysozyme nanoislands still maintain their bioactivity.

Summary and Conclusion

Each lysozyme protein molecule occupies an area $3 \times 5 = 15$ nm^2, assuming that the lysozyme is oriented with the long axis parallel to the surface. Thus, on the solution-prepared template, each protein island incorporates approximately 640 lysozyme molecules, while on the vapor-prepared template each protein island incorporates approximately 195 lysozyme molecules assuming that lysozyme molecules are closely packed. In terms of areal coverage, the former protein covers 27% of the surface area whereas for the latter the protein covers 7.5% of the surface area. On a 1×1 cm^2 protein nanoarray template, the amount of protein immobilized on the surface is 43 ng and 12 ng for the solution and vapor-prepared surfaces, respectively. These results demonstrate that arrays of lysozyme nanoislands can be utilized as a lysozyme antibody sensor. On the vapor-phase-prepared template, as few as 200 antibody molecules coat a single protein island and this can be easily detected with AFM.

In summary, by incorporating nanosphere lithography and surface silane chemistry, we have developed a method to fabricate hexagonal arrays of nanoscale protein islands over cm^2 regions while preserving the protein's bio-functionality. The island feature size is 60−120 nm, a comparable dimension to the SPM-based protein patterning methods. Although the nature of nanosphere lithography limits the pattern to a hexagonal pattern and ~30 μm single crystalline order, our method offers an economical solution for large-scale high-resolution protein patterning. By using nanospheres of different sizes, the area density of the protein array can be varied. This method could be readily adopted to the fabrication of wafer sized nanoarrays and possibly smaller islands by using nanospheres with smaller diameters.

Acknowledgment. We thank Masa Fukuto for insightful conversations. B.O. thanks the hospitality of the Stony Brook University Physics Department during the preparation of this manuscript. BNL is supported by the U.S. Department of Energy under Contract No. DE- AC02-98CH10886.

Supporting Information Available: AFM image of a typical nanosphere single crystal domain (Figure S1). Details on the solution-prepared protein nanoarrays, including the presence of highly ordered hexagonal arrays (Figure S2). This material is available free of charge via the Internet at http://pubs.acs.org.

LA051656E

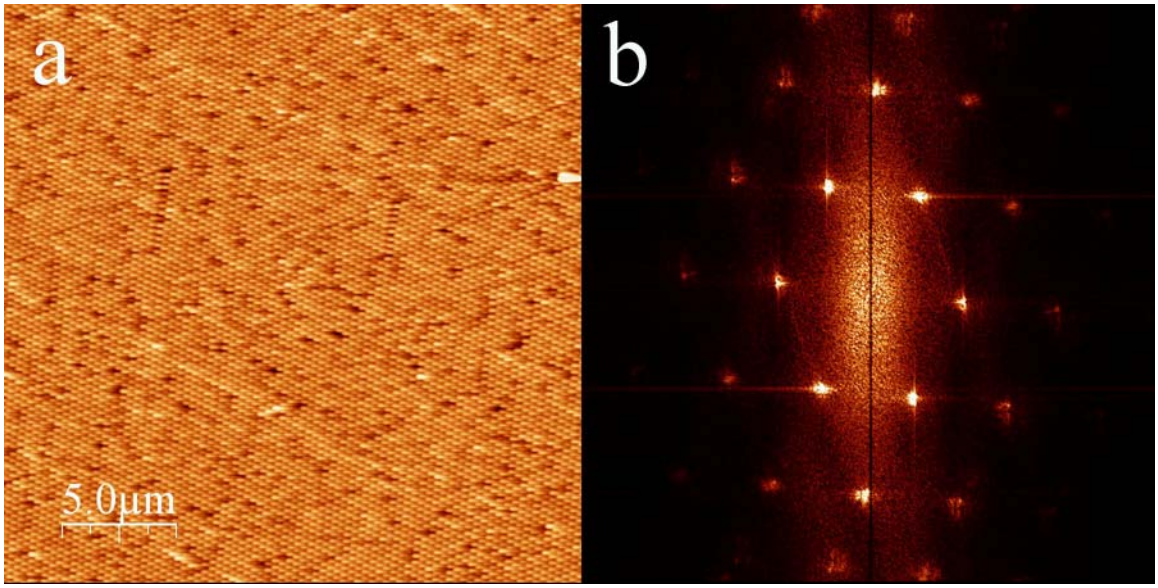

Figure S1 A typical 300 nm nanosphere monolayer surface on the UTS_{ox} substrate. Scan size 25x25 μm^2. Although the point defects are visible in the topography image, all the spheres in the image are in a single crystal domain. This is clearly shown in the FFT image (b).

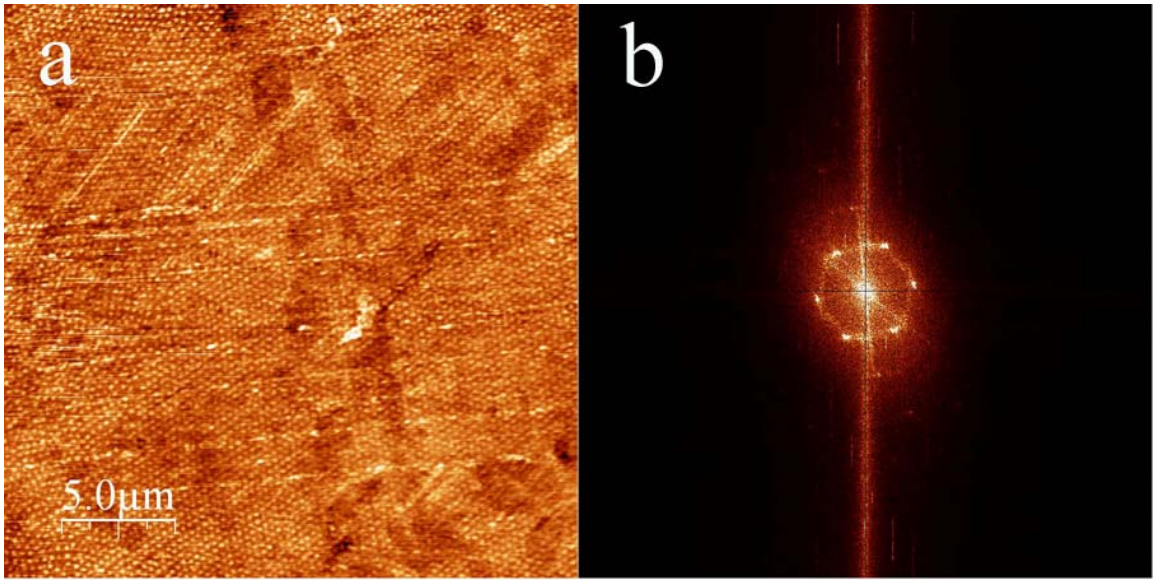

Figure S2 A typical lysozyme protein nano-array image on the solution prepared PEG-silane-UTS_{ox} template. Scan size 25x25 μm^2 (a). topography image (b) FFT transform image of (a).